Isı Bilimi ve Tekniği Dergisi, 40, 2, 251-265, 2020
J. of Thermal Science and Technology
©2020 TIBTD Printed in Turkey
ISSN 1300-3615
https://doi.org/10.47480/isibted.817013

THERMOECONOMIC ANALYSIS OF T56 TURBOPROP ENGINE UNDER DIFFERENT LOAD CONDITIONS

Dilek Nur OZEN*, Cuneyt UYSAL and Ozgur BALLI*****
*Corresponding author, Necmettin Erbakan University, Faculty of Engineering and Architecture, Mechanical Engineering Department, 42060, Konya, Turkey, dnozen@erbakan.edu.tr, ORCID: 0000-0002-8622-4990
**Karabuk University, TOBB Vocational School of Technical Sciences, Automotive Technologies Program, 78050, Karabuk, Turkey, cuneytuysal@karabuk.edu.tr, ORCID: 0000-0002-7986-1684
***First Air Maintenance Factory Directorate, Ministry of National Defence, Eskisehir, Turkey, balli07balli@yahoo.com, ORCID: 0000-0001-6465-8387

(Geliş Tarihi: 14.08.2019, Kabul Tarihi: 17.06.2020)

Abstract: In this study, T56 turboprop engine was theoretically modelled for 75% load, 100% load, military (MIL) mode, and Take-off mode conditions. For each load conditions, thermoeconomic analyses of T56 turboprop engine were performed to allocate the unit costs of shaft work and thrust and to determine exergy destruction cost rates for system equipment. In thermoeconomic analyses, Specific Exergy Costing (SPECO) and Modified Productive Structure Analysis (MOPSA) methods were used. MOPSA method gave higher unit cost values for shaft work and thrust compared to SPECO method. As a result, for Take-off mode, the unit cost of shaft work transferred to propeller was determined to be 78.87 $/GJ in SPECO method, while this value was calculated to be 84.68 $/GJ with MOPSA method. The unit cost of negentropy of T56 turboprop engine decreased with increasing in engine load and ranged from 14.98 $/GJ to 11.08 $/GJ. The exergy destruction cost rates obtained with MOPSA method for the system equipment were considerably lower than the results obtained with SPECO method. For instance, in Take-off mode, exergy destruction cost rate of combustion chamber was calculated to be 865.10 $/h in SPECO method, whereas it was calculated to be 247.94 $/h in MOPSA method. The exergoeconomic factor of overall system was determined to be 23.07% in SPECO method, and 54.16% in MOPSA method for Take-off mode.
Keywords: Aircraft engine, Exergy analysis, Thermoeconomics, MOPSA, SPECO.

T56 TURBOPROP MOTORUNUN FARKLI YÜK KOŞULLARI ALTINDA TERMOEKONOMİK ANALİZİ

Özet: Bu çalışmada, T56 turboprop motor %75, %100, askeri (MIL) ve kalkış (Take-off) yük koşulları için teorik olarak modellenmiştir. Her bir yük koşulunda, şaft işinin ve itme kuvvetinin birim maliyetlerinin ayrıklaştırılması ve sistem ekipmanlarının ekserji yıkım maliyetlerinin belirlenmesi için T56 turboprop motorun termoekonomik analizleri gerçekleştirilmiştir. Termoekonomik analizlerde, Specific Exergy Costing (SPECO) ve Modified Productive Structure Analysis (MOPSA) metotları kullanılmıştır. MOPSA metodu şaft işi ve itki kuvveti için SPECO metoduna kıyasla daha yüksek birim maliyetler vermektedir. Sonuç olarak, kalkış modu için, pervaneye iletilen şaft işinin birim maliyeti MOPSA metodu ile 84.68 $/GJ olarak hesaplanırken, SPECO metodunda 78.87 $/GJ olarak belirlenmiştir. T56 turboprop motorun negentropi birim maliyeti motor yükünün artmasıyla azalmaktadır ve 14.98 $/GJ'den 11.08 $/GJ'e kadar sıralanmaktadır. Sistem ekipmanları için MOPSA metodu ile elde edilen ekserji yıkımı maliyetleri SPECO metodu ile elde edilen sonuçlardan oldukça düşüktür. Örneğin, kalkış modu için, yanma odasının ekserji yıkımı maliyeti SPECO metodunda 865.10 $/h olarak hesaplanmıştır, oysa bu değer MOPSA metodunda 247.94 $/h olarak hesaplanmıştır. Toplam sistemin ekserjoekonomik faktörü, kalkış modu için, SPECO metodunda %23.07 ve MOPSA metodunda %54.16 olarak belirlenmiştir.
Anahtar Kelimler: Uçak motoru, Ekserji analizi, Termoekonomi, MOPSA, SPECO.

NOMENCLATURE

A	cross section area [m^2]
c	unit exergy cost [$/GJ]
c_P	specific heat capacity [kJ/kgK]
$\dot{C}$	exergy cost rate [$/h]
$\dot{Ex}$	exergy rate [kW]
f	exergoeconomic factor [%]
F	force [N]
g	gravitational acceleration [m/s^2]
h	specific enthalpy [kJ/kg]
LHV	lower heating value [kJ/kg]
$\dot{m}$	mass flow rate [kg/s]
P	pressure [kPa]
r	relative cost difference [%]
R	gas constant [kJ/kgK]

s	specific entropy [kJ/kgK]
$\dot{S}$	entropy rate [kJ/K]
T	temperature [K]
V	velocity [m/s]
z	height [m]
$\dot{Z}$	hourly capital investment cost rate [$/h]

Greek symbols

η	isentropic efficiency [%]
ψ	exergy efficiency [%]

Abbreviations

AC	air compressor
CC	combustion chamber
ED	exhaust duct
GT	gas turbine
GTMS	gas turbine mechanical shaft
MIL	military
MOPSA	modified productive structure analysis
PR	pressure ratio
RGB	reduction gearbox
SPECO	specific exergy costing

Subscripts

a	air
boun	boundary
BQ	external cooling stream
D	destruction
exh	exhaust
F	fuel
in	inlet
KE	kinetic exergy
M	mechanical
out	outlet
P	product
S	entropy
T	thermal
W	work
0	reference (dead) state

Superscripts

BQ	external cooling stream
CHE	chemical
KN	kinetic
M	mechanical
PT	potential
T	thermal
TM	thermomechanical

INTRODUCTION

Air transportation is generally a fast and time advantageous transportation technique compared to road and rail transportation, especially at long distances. The widespread of air transportation directly affects the social, cultural, political, and economical developments of societies. Therefore, the developments in air transportation are an important fact. The developments in air transportioncan also be evaluated in the aspect of economic and environmental. For this reason, the engines used in aircrafts an gain importance in the world. The operation of aircraft engines should be inexpensive, and this can also be provided with reduction of fuel consumption and product costs.

Thermoeconomics is an engineering branch that combines thermodynamics and economics. Thermoeconomic analysis allows obtaining the cost structures of thermal systems. It also allows to the cost allocation of products for multi-product systems. Designers/engineers can have information about the component that is the most responsible for cost ineffectiveness in any thermal system. By this way, thermoeconomic analysis can also be used for aircraft engines to understand their cost structures and to minimize their production costs. In literature, there are some studies related with thermoeconomic analysis of aircraft engines. For instance, Balli et al. (2008) realized exergetic and exergoeconomic analysis of a J69-T-25A jet engine used on T-37B/C series military training aircrafts. The exergy efficiency of jet engine was found to be 34.84% and the unit exergy cost of exhaust gases was obtained to be 70.956 $/GW. Balli and Hepbasli (2014) studied exergoeconomic, sustainability and environmental damage cost analyses of T56 turboprop engine for different power load conditions. The exergy destruction cost rate of overall system was calculated 774.96GJ/h, 947.24GJ/h, 985.85GJ/h and 1002.17GJ/h for 75%, 100%, military and take-off load conditions, respectively. In the calculation of exergy destruction cost, the unit cost of fuel (c_F) was used. Similarly, Balli (2019) obtained that the exergoeconomic factor of a GE90-115 high bypass turbofan engine was 70.23% when the c_F value was used. Turgut et al. (2009) studied the exergoeconomic analysis of an aircraft turbofan engine. In the calculation of exergy destruction cost rate, both the unit cost of fuel (c_F) and the unit cost of product (c_P) were used to show the limitation of exergy destruction cost rate. Similarly, Altuntas et al. (2012) used both the unit cost of fuel (c_F) and the unit cost of product (c_P) to calculate the exergy destruction cost rate of a piston-prop aircraft engines. They reported that the maximum exergy destruction cost rate was observed in taxiing. It was calculated to be 23.41 $/h at a fixed production and to be 2.96 $/h at a fixed fuel.

Literature survey presented above revealed that the unit cost of fuel (c_F) or the unit cost of product (c_P) have been used in the calculation of exergy destruction cost rate of aircraft engines. *Modified Productive Structure Analysis* (MOPSA) method, which is one of the thermoeconomic methods, allows assigning a separate unit cost in the calculation of exergy destruction cost rate. This unit cost is called as *the unit cost of negentropy* (c_s). Some studies have performed on the comparison of the usage of c_F and c_S values on the costing of exergy destruction rate. Uysal (2020) reported that the usage of c_F on the costing of exergy destruction rate can give

higher exergy destruction cost rate for any system equipment than that of overall system. This situation looks like unacceptable. Similarly, Uysal et al. (2020) reported that the usage of c_S gives considerably lower exergy destruction cost rate compared to the c_F. This situation directly affects the strategies to be developed to obtain a cost-effective system. For instance, according to the results obtained by Uysal et al. (2020), the usage of c_S can lead to reducing the investment costs for any equipment, while the usage of c_F can lead to reducing the exergy destruction cost rate for the same equipment. Haydargil and Abusoglu (2018) reported that MOPSA method investigates destructions more clearly compared to Specific Exergy Costing (SPECO), Exergetic Cost Theory (ECT) and Wonergy methods.

In the literature, MOPSA method has been applied to several thermal systems such as natural gas-fired electricity generating facility (Uysal, 2020), coal-fired power plant (Uysal and Kurt, 2017), gas turbine power plant (Kwak et al., 2003 and Bandpy and Ebrahimian,2006) gas turbine cogeneration system (Kim et al., 1998 and Kwak et al., 2004) biogas engine-powered cogeneration system (Haydargil and Abusoglu, 2018), combined supercritical CO_2 regenerative and organic Rankine cycle (Uysal et al., 2020), ocean thermal energy conversion system (Jung et al., 2016), air-cooled air conditioning system (Yoo et al., 2018), water-to-water heat pump system (Aksu et al., 2019), ground-source heat pump system (Kwak et al., 2014), geothermal district heating system (Kecebas,2013), binary geothermal power plant (Yilmaz, 2018), and fuel cells (Kwak et al., 2004, Seo et al., 2019). According to the best knowledge of authors, MOPSA method has not been applied to any aircraft engine.

In this paper, T56 turboprop engine was theoretically modelled for different load conditions (75% load, 100% load, military, and take-off modes). MOPSA method was applied to determine the product costs (shaft work for propeller and thrust). Moreover, the exergy destruction cost rate, relative cost difference, and exergoeconomic factor values of system equipment were calculated for each load conditions. At the same time, SPECO method was applied to the system. The results obtained with both MOPSA and SPECO methods were presented and compared.

MATERIAL AND METHOD

System Description

In general, T56 turboprop engines are a single-shaft turboprop engine with a 14-stage axial flow compressor driven by a four-stage turbine. The gearbox has two stages of gear reduction and features a propeller brake. T56 turboprop engines are widely used in military aircrafts (C-130A-H Hercules, E-2C/D Hawkeye, P-3C Orion, C-2A Greyhound etc.) and in commercial aircrafts (CV-580, CV-5800, L-100 Hercules, L-188 Electra, etc.) (Balle, 2016). A schematic diagram of a T56 turboprop engine is illustrated in Figure 1.

T56 turboprop engine consists of three main parts. These are the power section assembly, the torque meter assembly and the reduction gear assembly. The power section consists of an axial flow compressor, a combustion section, and a turbine. This section includes fuel, ignition, and cooling air systems. The torque meter assembly is located between the power section and the reduction gear section. The purpose of this section is to measure the shaft output of the power section and to transmit it to the reduction gear section. The reduction gear section changes the shaft speed from high rpm to low rpm for efficient propeller operation. Atmospheric air enters to air compressor (AC) and compressed air is transferred to combustion chamber (CC). After combustion process of fuel-air mixture in CC, exhaust gases are transferred to gas turbine (GT). After shaft work generation in GT, exhaust gases leaving from GT enter to exhaust duct (ED). Velocity of exhaust gases is increased in ED and exhaust gases are released to atmosphere. Exhaust gases leaving from ED with high velocity provide production of thrust. Some part of shaft

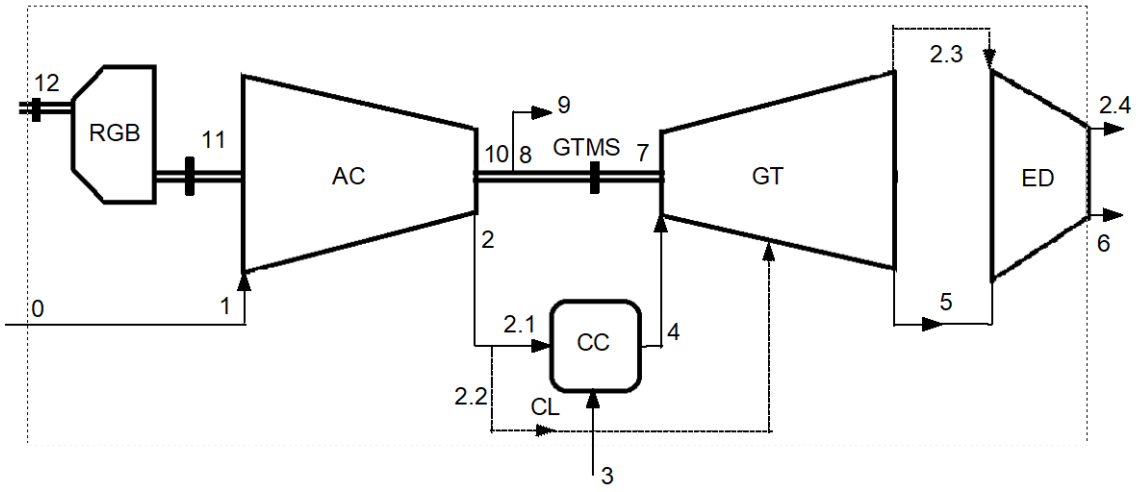

Figure 1. A schematic diagram of T56 turboprop engine

work generated in GT is used to drive AC and its remaining part is transferred to reduction gearbox (RGB). Shaft work in the exit of RGB is used to drive the propeller.

Exergy Analysis

When nuclear, magnetism, electricity and surface tension effects are ignored, total exergy rate for a flow of matter through a system can be expressed as follows:

$$\dot{E}x = \dot{E}x^{TM} + \dot{E}x^{CHE} + \dot{E}x^{KN} + \dot{E}x^{PT} \quad (1)$$

where the superscripts TM, CHE, KN and PT denote thermomechanical, chemical, kinetic, and potential exergies, respectively. Thermomechanical exergy can be expressed as follows:

$$\dot{E}x^{TM} = \dot{m}\left\{\begin{matrix} h(T,P) - h(T_0,P_0) \\ -T_0\left[s(T,P) - s(T_0,P_0)\right] \end{matrix}\right\} \quad (2)$$

Thermomechanical exergy can be divided into its thermal and mechanical components. Thermal and mechanical components of thermomechanical exergy can be formulated as follows, respectively:

$$\dot{E}x^{T} = \dot{m}\left\{\begin{matrix} h(T,P) - h(T_0,P) \\ -T_0\left[s(T,P) - s(T_0,P)\right] \end{matrix}\right\} \quad (3)$$

$$\dot{E}x^{M} = \dot{m}\left\{\begin{matrix} h(T_0,P) - h(T_0,P_0) \\ -T_0\left[s(T_0,P) - s(T_0,P_0)\right] \end{matrix}\right\} \quad (4)$$

For ideal gases, thermomechanical exergy can be expressed as follows:

$$\dot{E}x^{TM} = \dot{m}\left\{\begin{matrix} c_P\left[T - T_0 - T_0 \ln\left(\frac{T}{T_0}\right)\right] \\ +RT_0 \ln\left(\frac{P}{P_0}\right) \end{matrix}\right\} \quad (5)$$

In Equation 5, the first and second terms on the right-hand side express thermal and mechanical components of thermomechanical exergy. In this study, chemical exergy was taken into account in only combustion process. The chemical exergy rate of liquid fuels ($C_xH_yO_zS_\sigma$) can be calculated with following relation (Balli and Hepbasli, 2014):

$$\frac{\dot{E}x^{CHE}}{\dot{m}_F LHV} = 1.0401 + 0.01728\frac{y}{x} + 0.0432\frac{z}{x} + 0.2196\frac{\sigma}{x}\left(1 - 2.0628\frac{y}{x}\right) \quad (6)$$

Kinetic and potential exergies can be given as follows, respectively:

$$\dot{E}x^{KN} = \dot{m}\frac{V^2}{2} \quad (7)$$

$$\dot{E}x^{PT} = \dot{m}gz \quad (8)$$

The thrust produced by T56 turboprop engine can be calculated with using momentum equation as follows:

$$F = \dot{m}_{out}V_{out} - \dot{m}_{in}V_{in} + A_{out}P_{out} - A_{in}P_{in} \quad (9)$$

The kinetic exergy rate of the thrust produced by T56 turboprop engine can be expressed as follows (Balli and Hepbasli, 2013):

$$\dot{E}x^{KN} = \dot{m}_{exh}\frac{V_{exh}^2}{2000} \quad (10)$$

Exergy balance and exergy efficiency equations of a system can be written as follows, respectively:

$$\dot{E}x_D = \dot{E}x_F - \dot{E}x_P \quad (11)$$

$$\psi = \frac{\dot{E}x_P}{\dot{E}x_F} \quad (12)$$

where the F, P and D subscripts denote fuel, product, and destruction, respectively.

Thermoeconomic Analysis

There exist several methods for thermoeconomic analysis of thermal systems. These methods are based on completely different fundamentals and assumptions. Among these methods, SPECO and MOPSA are well-known and commonly used methods.

Specific Exergy Costing (SPECO)

SPECO method was introduced by Lazzaretto and Tsatsaronis (2006). This method aims to calculate the specific exergy cost of all states located in a system. Equation 13 gives the general cost balance equation of this method.

$$\sum\left(c_{out}\dot{E}x_{out}\right)_k + c_{W,k}\dot{W}_k = \sum\left(c_{in}\dot{E}x_{in}\right)_k + c_{q,k}\dot{E}x_{q,k} + \dot{Z}_k \quad (13)$$

With applying Equation 13 to each equipment of system, an equation set with a number of equations equal to the number of equipment is obtained. However, to be able to determine the specific exergy cost of all states located in the system, the number of equations should be equal to the number of states located in the system. For this reason, auxiliary equations are required. In SPECO method, auxiliary equations are written with *Fuel-Product Rule*. This rule is based on fuel and product definitions of system equipment. According to the *Fuel Rule*, the specific exergy cost of removed exergy from a stream defined as fuel in the equipment should be equal

to the average specific cost at which the removed exergy was supplied to the same stream in upstream components. According to the *Product Rule*, when a stream defined as product in the equipment is divided into parts, each stream has the same specific exergy cost. Fuel and Product definitions for the system equipment considered in this study were given in Table 1.

Table 1. Fuel and product exergy equations for the system equipment in SPECO method

Equipment	Fuel	Product
AC	$\dot{E}x_{10} - \dot{E}x_{11}$	$\dot{E}x_{2} - \dot{E}x_{1}$
CC	$\dot{E}x_{3} + \dot{E}x_{2,1}$	$\dot{E}x_{4}$
GT	$\left(\dot{E}x_{4} - \dot{E}x_{5}\right) + \left(\dot{E}x_{2,2} - \dot{E}x_{2,3}\right)$	$\dot{E}x_{7}$
ED	$\left(\dot{E}x_{5} - \dot{E}x_{6}\right) + \left(\dot{E}x_{2,3} - \dot{E}x_{2,4}\right)$	$\dot{E}x_{KE}$
GTMS	$\dot{E}x_{7}$	$\dot{E}x_{10}$
RGB	$\dot{E}x_{11}$	$\dot{E}x_{12}$

For this study, cost balance and auxiliary equations written with SPECO method were tabulated in Table 2. With considering fuel and product definition, Equation 13 can also be rewritten as follows:

$$c_{F,k}\dot{E}x_{F,k} + \dot{Z}_{k} = c_{P,k}\dot{E}x_{P,k} \qquad (14)$$

where $c_{F,k}$ and $c_{P,k}$ values express the specific exergy cost of fuel and product, respectively.

Modified Productive Structure Analysis (MOPSA)

Lozano and Valero (1993) proposed a method based on productive structure of thermal systems. Design and operation of thermal systems are strongly dependent on their productive structure. This method allows to disaggregate the system in productive and dissipative units. Moreover, it allows to divide exergy stream into its thermal, mechanical, and chemical components. Kim et al. (1998) developed an exergy-based cost balance equation with considering the method proposed by Lozano and Valero (1993). This cost balance equation was modified by Kwak et al. (2003) for the non-adiabatic equipment to reflect the exergy losses due to heat transfer and the resulting costs.

Thus, final version of method is called as *Modified Productive Structure Analysis* (MOPSA) and the general cost balance equation for this method can be given as follows:

$$\begin{aligned}&\dot{E}x^{CHE}c_{0} + \dot{E}x^{BQ}c_{BQ} + \left(\sum \dot{E}x_{in}^{T} - \sum \dot{E}x_{out}^{T}\right)c_{T} \\ &+ \left(\sum \dot{E}x_{in}^{M} - \sum \dot{E}x_{out}^{M}\right)c_{M} + T_{0}\left(\sum \dot{S}_{in} - \sum \dot{S}_{out}\right)c_{S} \\ &+ \dot{Z}_{k} = \dot{E}x^{W}c_{W}\end{aligned} \qquad (15)$$

MOPSA method is based on exergy costing without flow-stream cost calculation. In this method, thermomechanical exergy is divided into its thermal and mechanical components and a unit cost is assigned for these components. Moreover, a separate unit cost, which is called as the unit cost of negentropy, is assigned for exergy destruction term. With using Equation 15, an equation set with a number of equations equal to the number of equipment is obtained. For each equation, productive cost of equipment is defined as unknown. To be able to solve the equation set, the number of equations should be equal to the number of unknowns. Therefore, junctions are used when needed. Junctions are fictitious equipment where homogeneous productions of two or more equipment merge (Lozano and Valero, 1993). In addition, a unit cost balance equation can be written for system boundary. System boundary is responsible for entropy generation of overall system. The equation set obtained with MOPSA method for the system considered in this study is presented in Table 3. The specific exergy costs coloured as red in Table 3 are productive costs of equipment. Fuel and product definitions of system equipment show differences when the exergy streams are divided into their thermal and mechanical components. Table 4 represents fuel and product definitions for divided exergy stream. These terms will be used in MOPSA method.

Equation 15 can be rewritten as follows with considering fuel and product definitions

$$c_{F,k}\dot{E}x_{F,k} + c_{S,k}\dot{E}x_{D,k} + \dot{Z}_{k} = c_{P,k}\dot{E}x_{P,k} \qquad (16)$$

where $c_{S,k}$ is the unit cost of negentropy. As can be seen from Equations 14 and 16, the general cost balance equation of MOPSA is including exergy destruction cost rate, while that of SPECO has no information about exergy destruction cost rate.

Table 2. Cost balance and auxiliary equations for the system equipment in SPECO method

Component	Cost balance equation	Auxiliary equation
AC	$\dot{C}_{1} + \dot{C}_{10} + \dot{Z}_{AC} = \dot{C}_{2} + \dot{C}_{11}$	$c_{1} = 0, \quad c_{2} = c_{2,1} = c_{2,2}$
CC	$\dot{C}_{2,1} + \dot{C}_{3} + \dot{Z}_{CC} = \dot{C}_{4}$	$c_{3} = 25.20\$ / GJ$
GT	$\dot{C}_{4} + \dot{C}_{2,2} + \dot{Z}_{GT} = \dot{C}_{5} + \dot{C}_{2,3} + \dot{C}_{7}$	$c_{4} = c_{5}, \quad c_{2,2} = c_{2,3}$
ED	$\dot{C}_{2,3} + \dot{C}_{5} + \dot{Z}_{ED} = \dot{C}_{2,4} + \dot{C}_{6} + \dot{C}_{KE}$	$c_{5} = c_{6}, \quad c_{2,3} = c_{2,4}$
GTMS	$\dot{C}_{7} + \dot{Z}_{GTMS} = \dot{C}_{10}$	$c_{8} = c_{9} = c_{10} = c_{11}$
RGB	$\dot{C}_{11} + \dot{Z}_{RGB} = \dot{C}_{12}$	-

Thermoeconomic variables

Thermoeconomic variables are important parameters in the thermoeconomic evaluation and optimization of thermal systems. These variables may be ordered as: exergy destruction cost, exergoeconomic factor and relative cost difference.

In SPECO method, exergy destruction cost of any thermal system is calculated with using the unit cost of fuel (c_F) of thermal system. However, MOPSA method allows assigning the unit cost of negentropy (c_S) for exergy destruction. With considering these situations, exergy destruction cost rate for SPECO and MOPSA methods can be calculated as follows, respectively:

$$\dot{C}_{D,k} = c_{F,k}\dot{E}x_{D,k} \tag{17}$$

$$\dot{C}_{D,k} = c_{S,k}\dot{E}x_{D,k} \tag{18}$$

Table 3. Cost balance equations for the system equipment in MOPSA method

Equipment	Cost balance equation
AC	$\left(\dot{E}x_1^T - \dot{E}x_2^T\right)c_T + \left(\dot{E}x_1^M - \dot{E}x_2^M\right)c_{1M} + \left(\dot{E}x_{dest,AC}\right)c_S + \dot{Z}_{AC} = \left(\dot{E}x_{11}^W - \dot{E}x_{10}^W\right)c_W$
CC	$\dot{E}x_3^{CHE}c_0 + \left(\dot{E}x_{2.1}^T - \dot{E}x_4^T\right)c_{2T} + \left(\dot{E}x_{2.1}^M - \dot{E}x_4^M\right)c_M + \left(\dot{E}x_{dest,CC}\right)c_S + \dot{Z}_{CC} = 0$
GT	$\left(\dot{E}x_{2.2}^T + \dot{E}x_4^T - \dot{E}x_{2.3}^T - \dot{E}x_5^T\right)c_T + \left(\dot{E}x_{2.2}^M + \dot{E}x_4^M - \dot{E}x_{2.3}^M - \dot{E}x_5^M\right)c_M + \left(\dot{E}x_{dest,GT}\right)c_S + \dot{Z}_{GT} = \left(\dot{E}x_7^W\right)c_{3W}$
ED	$\left(\dot{E}x_{2.3}^T + \dot{E}x_5^T - \dot{E}x_{2.4}^T - \dot{E}x_6^T\right)c_T + \left(\dot{E}x_{2.3}^M + \dot{E}x_5^M - \dot{E}x_{2.4}^M - \dot{E}x_6^M\right)c_M + \left(\dot{E}x_{dest,ED}\right)c_S + \dot{Z}_{ED} = \left(\dot{E}x_{KE}\right)c_{4KE}$
GTMS	$\left(\dot{E}x_{dest,GTMES}\right)c_S + \dot{Z}_{GTMS} = \left(\dot{E}x_{10}^W - \dot{E}x_7^W\right)c_{5W}$
RGB	$\left(\dot{E}x_{dest,RGB}\right)c_S + \dot{Z}_{RGB} = \left(\dot{E}x_{12}^W - \dot{E}x_{11}^W\right)c_{6W}$
W-Junction	$\left(\dot{E}x_7^W + \dot{E}x_{10}^W - \dot{E}x_7^W + \dot{E}x_{12}^W - \dot{E}x_{11}^W\right)c_W - \left(\dot{E}x_7^W\right)c_{3W} - \left(\dot{E}x_{10}^W - \dot{E}x_7^W\right)c_{5W} - \left(\dot{E}x_{12}^W - \dot{E}x_{11}^W\right)c_{6W} = 0$
T-Junction	$\left(\dot{E}x_{2.1}^T - \dot{E}x_4^T\right)c_T - \left(\dot{E}x_{2.1}^T - \dot{E}x_4^T\right)c_{2T} = 0$
P-Junction	$\left(\dot{E}x_1^M - \dot{E}x_2^M\right)c_M - \left(\dot{E}x_1^M - \dot{E}x_2^M\right)c_{1M} = 0$
Boundary	$\left(\dot{E}x_6^T + \dot{E}x_{2.4}^T - \dot{E}x_1^T\right)c_T + \left(\dot{E}x_6^M + \dot{E}x_{2.4}^M - \dot{E}x_1^M\right)c_M - \dot{E}x_{12}^W c_W + \left(\dot{E}x_{dest,boun}\right)c_S + \dot{Z}_{boun} = 0$

Table 4. Fuel and product definitions for the system equipment in MOPSA method

Equipment	Fuel	Product
AC	$\dot{E}x_{10} - \dot{E}x_{11}$	$\left(\dot{E}x_2^T - \dot{E}x_1^T\right) + \left(\dot{E}x_2^M - \dot{E}x_1^M\right)$
CC	$\dot{E}x_3 + \left(\dot{E}x_{2.1}^M - \dot{E}x_4^M\right)$	$\left(\dot{E}x_4^T - \dot{E}x_{2.1}^T\right)$
GT	$\left(\dot{E}x_{2.2}^T + \dot{E}x_4^T - \dot{E}x_{2.3}^T - \dot{E}x_5^T\right) + \left(\dot{E}x_{2.2}^M + \dot{E}x_4^M - \dot{E}x_{2.3}^M - \dot{E}x_5^M\right)$	$\dot{E}x_7$
ED	$\left(\dot{E}x_{2.3}^T + \dot{E}x_5^T - \dot{E}x_{2.4}^T - \dot{E}x_6^T\right) + \left(\dot{E}x_{2.3}^M + \dot{E}x_5^M - \dot{E}x_{2.4}^M - \dot{E}x_6^M\right)$	$\dot{E}x_{KE}$
GTMS	$\dot{E}x_7$	$\dot{E}x_{10}$
RGB	$\dot{E}x_{11}$	$\dot{E}x_{12}$

Exergoeconomic factor can be defined as follows (Bejan, 1996):

$$f_k = \frac{\dot{Z}_k}{\dot{Z}_k + \dot{C}_{D,k}} \tag{19}$$

Exergoeconomic factor has a great importance to decide that one should focus on reducing investment costs or reducing exergy destruction to obtain cost-effective thermal system.

Relative cost difference can be expressed as follows (Bejan, 1996):

$$r_k = \frac{c_{P,k} - c_{F,k}}{c_{F,k}} \tag{20}$$

Relative cost difference expresses the relative increase in the average cost per exergy unit between fuel and product of the equipment (Bejan, 1996).

RESULTS AND DISCUSSIONS

In this study, thermoeconomic analysis of a T56 turboprop engine was performed. Four different load conditions were considered: 75% load condition, 100% load condition, military mode (MIL) and take-off mode. T56 turboprop engine was modelled theoretically. Exergy and thermoeconomic analyses of T56 turboprop engine were performed for all load conditions. In thermoeconomic analysis, Specific Exergy Costing (SPECO) and Modified Productive Structure Analysis (MOPSA) methods were used.

Operating parameters assumed in the theoretical modelling of system were tabulated in Table 5.

The following assumptions were made in the modelling of T56 turboprop engine:

- The system operates in steady-state and steady flow.
- Air and combustion gases behave like ideal gas.
- The combustion reaction is complete.
- JP-8 jet fuel is used as fuel.
- LHV value of JP-8 jet fuel is assumed to be 42800 kJ/kg.
- The compressor and gas turbine are considered as adiabatic.
- The kinetic exergies (except thrust) and potential exergies are negligible.
- Chemical exergies are considered in only combustion reaction.
- The velocity of air entering to the engine is assumed to be zero.
- Environmental (dead-state) temperature and pressure are assumed to be 298.15K and 93.6 kPa, respectively.

Table 5. Assumptions for main operating data of turboprop engine (Balli and Hepbasli, 2013)

Parameter	Value
T_0 (K)	298.15
P_0 (kPa)	93.6
$\dot{m}_1$ (kg/s)	14.75
$\dot{m}_{2.2}$ (kg/s)	1.475
PR (-)	9.45
P_5 (kPa)	95.35
P_6 (kPa)	94.87
η_{AC}	88%
η_{GT}	90%
η_{ED}	90%

Thermodynamic data obtained from theoretical model for each load condition were tabulated in Table 6-9, respectively.

Table 6. Thermodynamic data for the turboprop engine at 75% load condition

State	Matter	$\dot{m}$ (kg/s)	T (K)	P (kPa)	$E\dot{x}^T$ (GJ/h)	$E\dot{x}^M$ (GJ/h)	$E\dot{x}$ (GJ/h)
0	Air	-	298.15	93.60	-	-	-
1	Air	14.750	298.15	93.60	0.00	0.00	0.00
2	Air	14.750	594.8	884.50	5.07	10.31	15.37
2.1	Air	13.275	594.8	884.50	4.56	9.28	13.84
2.2	Cooling air	1.475	594.8	884.50	0.51	1.03	1.54
2.3	Cooling air	1.475	744.97	95.35	0.86	0.01	0.87
2.4	Cooling air	1.475	744.13	94.87	0.86	0.01	0.87
3	Fuel	0.235	298.15	220.64	-	-	38.67
4	Combustion gas	13.592	1156.2	858.00	25.56	9.36	34.92
5	Combustion gas	13.592	720.98	95.35	8.48	0.08	8.56
6	Combustion gas	13.592	720.16	94.87	8.46	0.06	8.51
7	Shaft power	-	-	-	-	-	24.06
8	Shaft power	-	-	-	-	-	23.58
9	Shaft power	-	-	-	-	-	0.15
10	Shaft power	-	-	-	-	-	23.19
11	Shaft power	-	-	-	-	-	6.80
12	Shaft power	-	-	-	-	-	6.67
(2.4+6)	Kinetic exergy	-	-	-	-	-	0.05

Table 7. Thermodynamic data for the turboprop engine at 100% load condition

State	Matter	$\dot{m}$ (kg/s)	T (K)	P (kPa)	$E\dot{x}^T$ (GJ/h)	$E\dot{x}^M$ (GJ/h)	$E\dot{x}$ (GJ/h)
0	Air	-	298.15	93.60	-	-	-
1	Air	14.750	298.15	93.60	0.00	0.00	0.00
2	Air	14.750	594.80	884.50	5.07	10.31	15.37
2.1	Air	13.275	594.80	884.50	4.56	9.28	13.84
2.2	Cooling air	1.475	594.80	884.50	0.51	1.03	1.54
2.3	Cooling air	1.475	814.82	95.35	1.27	0.01	1.28
2.4	Cooling air	1.475	813.92	94.87	1.27	0.01	1.28
3	Fuel	0.294	298.15	220.64	-	-	48.37
4	Combustion gas	13.569	1290.60	858.00	31.86	9.34	41.20
5	Combustion gas	13.569	814.82	95.35	11.72	0.08	11.80
6	Combustion gas	13.569	813.92	94.87	11.69	0.06	11.75
7	Shaft power	-	-	-	-	-	26.45
8	Shaft power	-	-	-	-	-	25.92
9	Shaft power	-	-	-	-	-	0.15
10	Shaft power	-	-	-	-	-	25.51
11	Shaft power	-	-	-	-	-	9.12
12	Shaft power	-	-	-	-	-	8.94
(2.4+6)	Kinetic exergy	-	-	-	-	-	0.06

Table 8. Thermodynamic data for the turboprop engine at MIL load condition

State	Matter	$\dot{m}$ (kg/s)	T (K)	P (kPa)	$E\dot{x}^T$ (GJ/h)	$E\dot{x}^M$ (GJ/h)	$E\dot{x}$ (GJ/h)
0	Air	-	298.15	93.60	-	-	-
1	Air	14.750	298.15	93.60	0.00	0.00	0.00
2	Air	14.750	594.80	884.50	5.07	10.31	15.37
2.1	Air	13.275	594.80	884.50	4.56	9.28	13.84
2.2	Cooling air	1.475	594.80	884.50	0.51	1.03	1.54
2.3	Cooling air	1.475	837.09	95.35	1.36	0.02	1.39
2.4	Cooling air	1.475	836.12	94.87	1.36	0.02	1.38
3	Fuel	0.309	298.15	220.64	-	-	50.84
4	Combustion gas	13.584	1322.30	858.00	33.45	9.35	42.80
5	Combustion gas	13.584	837.09	95.35	12.56	0.08	12.64
6	Combustion gas	13.584	836.12	94.87	12.53	0.06	12.58
7	Shaft power	-	-	-	-	-	27.05
8	Shaft power	-	-	-	-	-	26.51
9	Shaft power	-	-	-	-	-	0.15
10	Shaft power	-	-	-	-	-	26.10
11	Shaft power	-	-	-	-	-	9.71
12	Shaft power	-	-	-	-	-	9.52
(2.4+6)	Kinetic exergy	-	-	-	-	-	0.06

According to Table 6-9, the net shaft power transferred to propeller was obtained to be 6.67 GJ/h for 75% load, 8.94 GJ/h for 100% load, 9.52 GJ/h for MIL mode, and 9.80 GJ/h for Take-off load. In addition, the kinetic exergy due to thrust was slightly increased with increase in engine load. Table 10-13 present the results of exergy balance of system equipment for each load condition, respectively.

As expected, the highest exergy destruction rate was observed for CC. The $E\dot{x}_D$ value of CC was calculated to be 17.59 GJ/h for 75% load, 21.01 GJ/h for 100% load (20.95 GJ/h in MOPSA), 21.88 GJ/h for MIL mode (21.78 GJ/h in MOPSA), and 22.39 GJ/h for Take-off mode. Similarly, the lowest exergy efficiency was obtained for CC. According to the fuel and product definition of SPECO, the exergy efficiency of CC was calculated to be 66.50% for 75% load, 66.23% for 100% load, 66.17% for MIL mode, and 66.08% for Take-off mode. When fuel and product definitions for MOPSA were used, the exergy efficiency of CC was obtained to be 54.42% for 75% load, 56.63% for 100% load, 56.90% for MIL mode, and 57.00% for Take-off mode.

Table 9. Thermodynamic data for the turboprop engine at Take-off load condition

State	Matter	$\dot{m}$ (kg/s)	T (K)	P (kPa)	$E\dot{x}^{T}$ (GJ/h)	$E\dot{x}^{M}$ (GJ/h)	$E\dot{x}$ (GJ/h)
0	Air	-	298.15	93.60	-	-	-
1	Air	14.750	298.15	93.60	0.00	0.00	0.00
2	Air	14.750	594.80	884.50	5.07	10.31	15.37
2.1	Air	13.275	594.80	884.50	4.56	9.28	13.84
2.2	Cooling air	1.475	594.80	884.50	0.51	1.03	1.54
2.3	Cooling air	1.475	847.94	95.35	1.41	0.01	1.42
2.4	Cooling air	1.475	847.01	94.87	1.41	0.01	1.41
3	Fuel	0.317	298.15	220.64	-	-	52.16
4	Combustion gas	13.592	1337.5	858.00	34.25	9.36	43.61
5	Combustion gas	13.592	847.94	95.35	12.99	0.08	13.06
6	Combustion gas	13.592	847.01	94.87	12.95	0.06	13.01
7	Shaft power	-	-	-	-	-	27.35
8	Shaft power	-	-	-	-	-	26.80
9	Shaft power	-	-	-	-	-	0.15
10	Shaft power	-	-	-	-	-	26.39
11	Shaft power	-	-	-	-	-	10.00
12	Shaft power	-	-	-	-	-	9.80
(2.4+6)	Kinetic exergy	-	-	-	-	-	0.06

Table 10. Exergetic values of system equipment at 75% load condition

Equipment	SPECO				MOPSA			
	$E\dot{x}_F$ (GJ/h)	$E\dot{x}_P$ (GJ/h)	$E\dot{x}_D$ (GJ/h)	ψ (%)	$E\dot{x}_F$ (GJ/h)	$E\dot{x}_P$ (GJ/h)	$E\dot{x}_D$ (GJ/h)	ψ (%)
AC	16.39	15.37	1.02	93.77	16.39	15.37	1.02	93.77
CC	52.51	34.92	17.59	66.50	38.59	21.00	17.59	54.42
GT	27.03	24.06	2.97	89.01	27.03	24.06	2.97	89.01
ED	0.052	0.05	0.002	96.15	0.052	0.05	0.002	96.15
GTMS	24.06	23.19	0.87	96.38	24.06	23.19	0.87	96.38
RGB	6.80	6.67	0.13	98.08	6.80	6.67	0.13	98.08

Table 11. Exergetic values of system equipment at 100% load condition

Equipment	SPECO				MOPSA			
	$E\dot{x}_F$ (GJ/h)	$E\dot{x}_P$ (GJ/h)	$E\dot{x}_D$ (GJ/h)	ψ (%)	$E\dot{x}_F$ (GJ/h)	$E\dot{x}_P$ (GJ/h)	$E\dot{x}_D$ (GJ/h)	ψ (%)
AC	16.39	15.37	1.02	93.77	16.39	15.37	1.02	93.77
CC	62.21	41.20	21.01	66.23	48.31	27.36	20.95	56.63
GT	29.66	26.45	3.21	89.17	29.66	26.45	3.21	89.17
ED	0.058	0.057	0.001	98.27	0.058	0.057	0.001	98.27
GTMS	26.45	25.51	0.94	96.45	26.45	25.51	0.94	96.45
RGB	9.12	8.94	0.18	98.03	9.12	8.94	0.18	98.03

Table 12. Exergetic values of system equipment at MIL load condition

Equipment	SPECO				MOPSA			
	$E\dot{x}_F$ (GJ/h)	$E\dot{x}_P$ (GJ/h)	$E\dot{x}_D$ (GJ/h)	ψ (%)	$E\dot{x}_F$ (GJ/h)	$E\dot{x}_P$ (GJ/h)	$E\dot{x}_D$ (GJ/h)	ψ (%)
AC	16.39	15.37	1.02	93.77	16.39	15.37	1.02	93.77
CC	64.68	42.80	21.88	66.17	50.77	28.89	21.78	56.90
GT	30.31	27.05	3.26	89.24	30.31	27.05	3.26	89.24
ED	0.07	0.06	0.01	85.71	0.07	0.06	0.01	85.71
GTMS	27.05	26.10	0.95	96.49	27.05	26.10	0.95	96.49
RGB	9.71	9.52	0.19	98.04	9.71	9.52	0.19	98.04

Table 13. Exergetic values of system equipment at Take-off load condition

Equipment	SPECO				MOPSA			
	$\dot{E}x_F$ (GJ/h)	$\dot{E}x_P$ (GJ/h)	$\dot{E}x_D$ (GJ/h)	ψ (%)	$\dot{E}x_F$ (GJ/h)	$\dot{E}x_P$ (GJ/h)	$\dot{E}x_D$ (GJ/h)	ψ (%)
AC	16.39	15.37	1.02	93.77	16.39	15.37	1.02	93.77
CC	66	43.61	22.39	66.08	52.08	29.69	22.39	57.00
GT	30.67	27.35	3.32	89.18	30.67	27.35	3.32	89.18
ED	0.062	0.058	0.004	93.55	0.062	0.058	0.004	93.55
GTMS	27.35	26.39	0.96	96.49	27.35	26.39	0.96	96.49
RGB	10.00	9.80	0.20	98.00	10.00	9.80	0.20	98.00

Table 14. The correlations for hourly capital investment cost rates of system equipment

Equipment	Correlation
AC (Sahu et al., 2017)	$\dot{Z} = \frac{25.65\dot{m}_{a,in}}{\left(0.995 - \frac{P_{out}}{P_{in}}\right)}\left[1+\exp\left(0.018T_{out} - 26.4\right)\right]$
CC (Sahu et al., 2017)	$\dot{Z} = \frac{39.5\dot{m}_{a,in}}{\left(0.9-\eta_{AC}\right)}\frac{P_{out}}{P_{in}}\ln\left(\frac{P_{out}}{P_{in}}\right)$
GT (Sahu et al., 2017)	$\dot{Z} = \frac{266.3\dot{m}_{g,out}}{\left(0.92-\eta_{GT}\right)}\ln\left(\frac{P_{in}}{P_{out}}\right)\left[1+\exp\left(0.036T_{in} - 54.4\right)\right]$
ED	adapted from Reference (Balli and Hepbasli, 2014)
GTMS	adapted from Reference (Balli and Hepbasli, 2014)
RGB	adapted from Reference (Balli and Hepbasli, 2014)

The correlations used to calculate hourly capital investment cost of system equipment were tabulated in Table 14. The results obtained with SPECO method for specific exergy cost and cost flow rate of states located in the system were given in Table 15

.

Table 15. The specific exergy cost and cost flow rates obtained with SPECO method for the system states

	75% load		100% load		MIL load		Take-off load	
State no	c ($/GJ)	$\dot{C}$ ($/h)	c ($/GJ)	$\dot{C}$ ($/h)	c ($/GJ)	$\dot{C}$ ($/h)	c ($/GJ)	$\dot{C}$ ($/h)
1	0	0	0	0	0	0	0	0
2	104.8	1372	92.29	1419	90.02	1384	89.27	1372
2.1	104.8	1451	92.29	1277	90.02	1246	89.27	1236
2.2	104.8	161.4	92.29	142.1	90.02	138.6	89.27	137.5
2.3	104.8	91.18	92.29	118.1	90.02	125.1	89.27	126.8
2.4	104.8	91.18	92.29	118.1	90.67	125.1	89.91	126.8
3	25.2	974.5	25.2	1219	25.2	1281	25.2	1314
4	69.55	2429	60.68	2500	59.14	2531	58.57	2554
5	69.55	595.4	60.68	716.1	59.14	747.5	58.57	764.9
6	69.55	591.9	60.68	713	59.14	743.9	58.57	762
7	84.21	2026	72.98	1930	70.96	1920	70.3	1923
8	87.81	2071	76.07	1972	73.94	1960	73.24	1963
9	87.81	13.17	76.07	11.41	73.94	11.09	73.24	10.99
10	87.81	2036	76.07	1941	73.94	1930	73.24	1933
11	87.81	597.1	76.07	693.8	73.94	717.9	73.24	732.4
12	95.6	637.7	82.14	734.3	79.67	758.5	78.87	772.9
KE	394.2	19.71	338	19.26	329.6	19.78	330.3	19.16

According to the results obtained with SPECO, the specific exergy cost of net shaft work transferred to propeller was 95.6 $/GJ for 75% load, 82.14 $/GJ for 100% load, 79.67 $/GJ for MIL load, and 78.87 $/GJ for Take-off mode. It was also said that the specific exergy cost of net shaft work transferred to propeller decreased with increase in engine load. The specific exergy cost of thrust was determined to be 394.2 $/GJ for 75% load, 338 $/GJ for 100% load, 329.6 $/GJ for MIL load, and 330.3 $/GJ for Take-off mode.

The results obtained with MOPSA method for productive costs were given in Table 16.

According to Table 16, the unit cost of net shaft work transferred to propeller was decreased with increase in engine load. The unit cost of net shaft work transferred to propeller was calculated to be 98.88 $/GJ for 75% load, 87.45 $/GJ for 100% load, 85.42 $/GJ for MIL load, and 84.68 $/GJ for Take-off mode. Similarly, the unit cost of thrust was determined to be 416.38 $/GJ for 75% load, 366.67 $/GJ for 100% load, 340.90 $/GJ for MIL load, and 354.86 $/GJ for Take-off mode. The unit cost of negentropy for the system was decreased with increasing engine load. The unit cost of negentropy was calculated to be 14.98 $/GJ for 75% load, 11.99 $/GJ for 100% load, 11.28 $/GJ for MIL load, and 11.08 $/GJ for Take-off mode.

The results obtained with MOPSA for the unit cost of net shaft work transferred to propeller were higher compared to the results obtained with SPECO. It is due to that the exergy destruction cost rate is taken into account in MOPSA method, while it is not considered in SPECO method.

The cost flow rates of turboprop engine for each load condition considered in this study were given in Table 17-20, respectively. In addition, Figure 2 shows the productive structure of system.

Table 16. The productive costs of system equipment obtained with MOPSA method

Parameter	75% load	100% load	MIL	Take-off
c_{1M}	155.985	137.193	133.860	132.667
c_{2T}	33.414	35.256	35.607	35.689
c_{3W}	93.276	82.333	80.388	79.688
c_{4KE}	416.378	366.670	340.896	354.861
c_{5W}	3.258	1.180	0.675	0.569
c_{6W}	283.134	210.364	197.572	191.784
c_{W}	98.881	87.447	85.415	84.677
c_{T}	33.414	35.256	35.607	35.689
c_{M}	155.985	137.193	133.860	132.667
c_{S}	14.981	11.989	11.279	11.076

Table 17. The cost flow rates of T56 turboprop engine for 75% load condition.

Equipment	$\dot{C}_0$ ($/h)	$\dot{C}_T$ ($/h)	$\dot{C}_M$ ($/h)	$\dot{C}_{KE}$ ($/h)	$\dot{C}_W$ ($/h)	$\dot{C}_D$ ($/h)	$\dot{Z}$ ($/h)
AC	0	− 169.28	− 1607.72	0	1620.46	− 15.20	171.75
CC	974.41	− 701.63	− 13.14	0	0	− 263.44	3.80
GT	0	558.68	1607.32	0	− 2243.99	− 44.45	122.44
ED	0	0.92	3.78	− 20.91	0	− 0.02	16.23
GTMS	0	0	0	0	2.85	− 12.99	10.14
RGB	0	0	0	0	− 38.52	− 2.04	40.56
Boundary	0	311.31	9.75	0	− 659.21	338.14	0
Overall System	974.41	0	0	− 20.91	− 1318.41	0	364.91

Table 18. The cost flow rates of T56 turboprop engine for 100% load condition.

Equipment	$\dot{C}_0$ ($/h)	$\dot{C}_T$ ($/h)	$\dot{C}_M$ ($/h)	$\dot{C}_{KE}$ ($/h)	$\dot{C}_W$ ($/h)	$\dot{C}_D$ ($/h)	$\dot{Z}$ ($/h)
AC	0	− 178.62	− 1414.04	0	1433.07	− 12.17	171.75
CC	1219.05	− 962.41	− 8.65	0	0	− 251.94	3.95
GT	0	682.82	1410.72	0	− 2177.43	− 38.40	122.29
ED	0	1.20	3.32	− 20.73	0	− 0.02	16.23
GTMS	0	0	0	0	1.11	− 11.25	10.14
RGB	0	0	0	0	− 38.37	− 2.19	40.56
Boundary	0	457.02	8.64	0	− 781.62	315.96	0
Overall System	1219.05	0	0	− 20.73	− 1563.23	0	364.92

Table 19. The cost flow rates of T56 turboprop engine for MIL mode.

Equipment	$\dot{C}_0$ ($/h)	$\dot{C}_T$ ($/h)	$\dot{C}_M$ ($/h)	$\dot{C}_{KE}$ ($/h)	$\dot{C}_W$ ($/h)	$\dot{C}_D$ ($/h)	$\dot{Z}$ ($/h)
AC	0	− 180.39	− 1379.68	0	1399.78	− 11.45	171.75
CC	1281.24	− 1028.81	− 9.75	0	0	− 246.75	4.07
GT	0	713.36	1375.74	0	− 2174.87	− 36.74	122.51
ED	0	1.43	3.25	− 20.87	0	− 0.04	16.23
GTMS	0	0	0	0	0.65	− 10.79	10.14
RGB	0	0	0	0	− 38.37	− 2.19	40.56
Boundary	0	494.41	10.45	0	− 812.81	307.95	0
Overall System	1281.24	0	0	− 20.87	− 1625.63	0	365.25

The cost flow rate of shaft work transferred to propeller increases with increase in load condition. The cost flow rate of shaft work generated by the system is calculated to be 1318.41 $/h, 1563.23 $/h, 1625.63 $/h and 1659.17 $/h for 75% load, 100% load, MIL and Take-off modes, respectively. Similarly, the cost flow rate of thrust is found to be 20.91 $/h, 20.73 $/h, 20.87 $/h and 20.75 $/h for all load conditions considered in this study, respectively. Tables 21-24 show the results of thermoeconomic variables obtained with using both SPECO and MOPSA methods. According to each method, CC was the most responsible equipment for exergy destruction cost rate at each engine load. For SPECO method, exergy destruction cost rate of CC was obtained to be 812.4 $/h for 75% load, 843.1 $/h for 100% load, 854.8 $/h for MIL load, and 865.1 $/h for Take-off load. In MOPSA method, these values were determined to be 263.44 $/h for 75% load, 251.94 $/h for 100% load, 246.75 $/h for MIL mode, and 247.94 $/h for Take-off mode.

In SPECO method, exergy destruction cost rate of overall system was determined to be 1195.96 $/h for 75% load, 1198.73 $/h for 100% load, 1205.49 $/h for MIL load, and 1216.93 $/h for Take-off load. According to the results obtained with MOPSA, exergy destruction cost rate of overall system was found to be 338.14 $/h for 75% load, 315.96 $/h for 100% load, 307.95 $/h for MIL mode, and 308.85 $/h for Take-off mode.

Table 20. The cost flow rates of T56 turboprop engine for Take-off mode.

Equipment	$\dot{C}_0$ ($/h)	$\dot{C}_T$ ($/h)	$\dot{C}_M$ ($/h)	$\dot{C}_{KE}$ ($/h)	$\dot{C}_W$ ($/h)	$\dot{C}_D$ ($/h)	$\dot{Z}$ ($/h)
AC	0	− 180.81	− 1367.38	0	1387.69	− 11.24	171.75
CC	1314.42	− 1059.66	− 10.97	0	0	− 247.94	4.16
GT	0	726.77	1366.77	0	− 2179.48	− 36.73	122.67
ED	0	1.34	3.22	− 20.75	0	− 0.04	16.23
GTMS	0	0	0	0	0.55	− 10.69	10.14
RGB	0	0	0	0	− 38.35	− 2.21	40.56
Boundary	0	512.37	8.37	0	− 829.59	308.85	0
Overall System	1314.42	0	0	− 20.75	− 1659.17	0	365.51

Table 21. Thermoeconomic variables of system equipment for 75% load conditions

Component	SPECO (S)		MOPSA (M)			$\dot{Z}$ ($/h)	S	M	S	M	S	M
	c_F ($/GJ)	c_P ($/GJ)	c_F ($/GJ)	c_P ($/GJ)	c_S ($/GJ)		$\dot{C}_{D,k}$ ($/h)	$\dot{C}_{D,k}$ ($/h)	r_k (%)	r_k (%)	f_k (%)	f_k (%)
AC	87.81	104.8	98.88	115.63	14.98	171.75	89.56	15.20	19.36	16.94	65.73	91.87
CC	46.18	69.55	24.91	33.41	14.98	3.80	812.4	263.44	50.61	34.12	0.46	1.42
GT	70.43	84.21	80.11	93.28	14.98	122.44	209.2	44.45	19.57	16.44	36.92	73.37
ED	66.88	394.2	88.63	416.38	14.98	16.23	0.1338	0.02	489.4	369.80	99.18	99.88
GTMS	84.21	87.81	93.28	96.65	14.98	10.14	73.26	12.99	4.27	3.61	12.16	43.84
RGB	87.81	95.6	91.33	98.88	14.98	40.56	11.41	2.04	8.87	8.27	78.04	95.21
Overall	25.20	-	25.20	-	14.98	364.91	1195.96	338.14	-	-	23.38	51.90

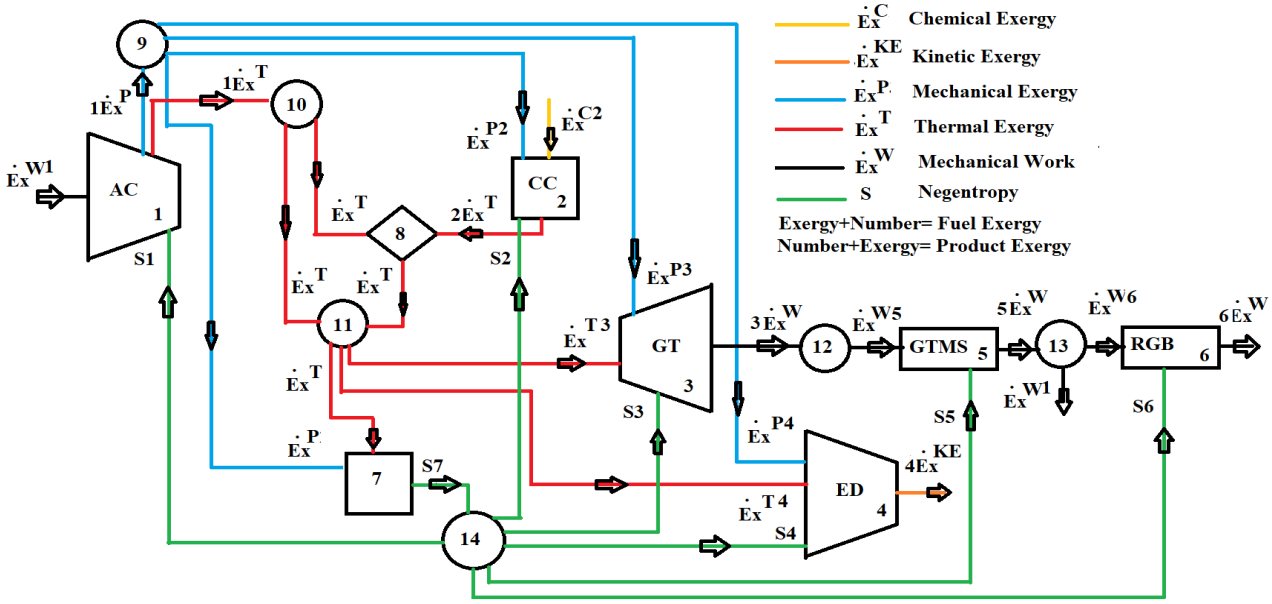

Figure 2. Productive structure of T56 turboprop engine

Table 22. Thermoeconomic variables of system equipment for 100% load conditions

Component	SPECO (S)		MOPSA (M)			$\dot{Z}$ ($/h)	S	M	S	M	S	M
	c_F ($/GJ)	c_P ($/GJ)	c_F ($/GJ)	c_P ($/GJ)	c_S ($/GJ)		$\dot{C}_{D,k}$ ($/h)	$\dot{C}_{D,k}$ ($/h)	r_k (%)	r_k (%)	f_k (%)	f_k (%)
AC	76.07	92.29	87.45	103.59	11.99	171.75	77.59	12.17	21.33	18.46	68.88	93.38
CC	40.13	60.68	24.53	35.26	11.99	3.80	843.1	251.94	51.23	43.74	0.47	1.54
GT	60.96	72.98	70.59	82.33	11.99	122.44	195.7	38.40	19.72	16.63	38.46	76.10
ED	52.31	338	80.87	366.67	11.99	16.23	0.05231	0.02	546	353.41	99.68	99.88
GTMS	72.98	76.07	82.33	85.32	11.99	10.14	68.6	11.25	4.23	3.63	12.88	47.41
RGB	76.07	82.14	81.51	87.45	11.99	40.56	13.69	2.19	7.98	7.29	74.76	94.88
Overall	25.20	-	25.20	-	11.99	364.91	1198.73	315.96	-	-	23.33	53.59

Table 23. Thermoeconomic variables of system equipment for MIL mode

Component	SPECO (S)		MOPSA (M)			$\dot{Z}$ ($/h)	S	M	S	M	S	M
	c_F ($/GJ)	c_P ($/GJ)	c_F ($/GJ)	c_P ($/GJ)	c_S ($/GJ)		$\dot{C}_{D,k}$ ($/h)	$\dot{C}_{D,k}$ ($/h)	r_k (%)	r_k (%)	f_k (%)	f_k (%)
AC	73.94	90.02	85.42	101.47	11.28	171.75	75.41	11.45	21.75	18.79	69.49	93.75
CC	39.07	59.14	25.04	35.61	11.28	3.80	854.8	246.75	51.36	42.21	0.47	1.62
GT	59.29	70.96	68.91	80.39	11.28	122.44	193.3	36.74	19.69	16.66	38.79	76.93
ED	50.69	329.6	60.91	340.90	11.28	16.23	0.5069	0.04	550.3	459.68	96.97	99.75
GTMS	70.96	73.94	80.39	83.29	11.28	10.14	67.42	10.79	4.18	3.61	13.07	48.45
RGB	73.94	79.67	79.79	85.42	11.28	40.56	14.05	2.19	7.76	7.06	74.28	94.88
Overall	25.20	-	25.20	-	11.28	364.91	1205.49	307.95	-	-	23.24	54.23

Table 24. Thermoeconomic variables of system equipment for Take-off mode

Component	SPECO (S)		MOPSA (M)			$\dot{Z}$ ($/h)	S	M	S	M	S	M
	c_F ($/GJ)	c_P ($/GJ)	c_F ($/GJ)	c_P ($/GJ)	c_S ($/GJ)		$\dot{C}_{D,k}$ ($/h)	$\dot{C}_{D,k}$ ($/h)	r_k (%)	r_k (%)	f_k (%)	f_k (%)
AC	73.24	89.27	84.68	100.74	11.08	171.75	74.7	11.24	21.89	18.97	69.69	93.86
CC	38.64	58.57	25.03	35.69	11.08	3.80	865.1	247.94	51.59	42.59	0.48	1.65
GT	58.69	70.3	68.26	79.69	11.08	122.44	194.8	36.73	19.78	16.74	38.63	76.96
ED	47.23	330.3	70.84	354.86	11.08	16.23	0.1889	0.04	599.40	400.93	98.85	99.75
GTMS	70.3	73.24	79.69	82.57	11.08	10.14	67.49	10.69	4.18	3.61	13.06	48.68
RGB	73.24	78.87	79.15	84.68	11.08	40.56	14.65	2.21	7.69	6.99	73.47	94.83
Overall	25.20	-	25.20	-	11.08	364.91	1216.93	308.85	-	-	23.07	54.16

When exergoeconomic factor was considered, both methods lead to the same modification strategy for all system equipment except GT. In SPECO method, exergoeconomic factor values obtained for GT was 36.92% for 75% load, 38.46% for 100% load, 38.79% for MIL mode, and 38.63% for Take-off mode. This means that one should focus on reducing exergy destruction cost rate of GT to obtain a cost-effective system. However, in MOPSA method, exergoeconomic factor of GT was calculated to be 73.37% for 75% load, 76.10% for 100% load, 76.93% for MIL mode, and 76.96% for Take-off mode. According to the results obtained with MOPSA method, one should focus on reducing the capital investment cost of GT for a cost-effective system. Exergoeconomic factor of overall system was determined to be 23.38% for 75% load, 23.33% for 100% load, 23.24% for MIL mode, and 23.07% for Take-off mode in SPECO method. In MOPSA method, exergoeconomic factor of overall system was calculated to be 51.90% for 75% load, 53.59% for 100% load, 54.23% for MIL mode, and 54.16% for Take-off mode.

SPECO and MOPSA methods gave different results for exergy destruction cost rates due to that they were based on different approaches to calculate the exergy destruction cost rate. The exergy destruction cost rates obtained with MOPSA were considerably lower compared the results obtained with SPECO. It is due to that the $c_{S,k}$ values were lower than the $c_{F,k}$ values. The differences on exergy destruction cost rates directly affect the exergoeconomic factor values. Although the same facts to develop modification strategies were obtained for each method, some differences could be observed. For instance, in this study, both methods proposed exactly opposite strategy for GT. SPECO proposed to reduce the exergy destruction cost rate to obtain cost-effective system, while MOPSA proposed to reduce the investment cost rate for the same equipment. According to the results obtained by Uysal (2020) and Uysal et al. (2020), the results obtained for exergy destruction cost rate obtained with MOPSA are more trustable compared to the results obtained by SPECO.

CONCLUSION

In this study, T56 turboprop engine was theoretically modelled for 75% load, 100% load, MIL mode, and Take-off mode conditions. Thermoeconomic analyses of T56 turboprop engine were performed with using SPECO and MOPSA methods.

The unit costs of shaft work transferred to propeller and thrust were higher in MOPSA method compared to the results obtained with SPECO method. It is due to that exergy destruction costs were considering in general cost balance equation of MOPSA method. However, the general cost balance equation of SPECO method has no information for exergy destruction cost rates.

MOPSA method gave lower values for exergy destruction cost rate of system equipment compared to SPECO method. This was due to that the unit cost of negentropy value of system was lower than the unit cost of fuel of system equipment. This differences in results can lead designers/engineers to develop exactly opposite strategies. For this reason, further studies can be performed on costing of exergy destruction. Such studies will also be helpful for theoretical unification of the different methodologies of thermoeconomic analysis.

REFERENCES

Altuntas, O., Karakoc, T. H. and Hepbasli, A., 2012, Exergetic, exergoeconomic and sustainability assessment of piston-prop aircraft engine. *Int J Therm Sci Technol, 32,* 133-43.

Aksu, B., 2019, Thermoeconomic Analysis Of A Water To Water Heat Pump Under Different Condenser And Evaporator Conditions. *Journal of Thermal Engineering*, *5*(3), 198-209.

Balle, J.K.O., 2016, About the Rolls-Royce T56, Forecast International.

Balli, O., 2019, Thermodynamic, thermoeconomic and environmental performance analyses of a high bypass

turbofan engine used on commercial aircrafts. *Sakarya Üniversitesi Fen Bilimleri Enstitüsü Dergisi*, *23*(3), 453-461.

Balli, O., Aras, H., Aras, N. and Hepbasli, A., 2008, Exergetic and exergoeconomic analysis of an Aircraft Jet Engine (AJE). *International Journal of Exergy*, *5*(5), 567.

Balli, O. and Hepbasli, A., 2013, Energetic and exergetic analyses of T56 turboprop engine. *Energy conversion and management*, *73*, 106-120.

Balli, O. and Hepbasli, A., 2014, Exergoeconomic, sustainability and environmental damage cost analyses of T56 turboprop engine. *Energy*, *64*, 582-600.

Bejan, A., Tsatsaronis, G. and Moran, M., 1996, Thermal Design and Optimization John Wiley and Sons. *Inc. New York*.

Gorji-Bandpy, M. and Ebrahimian, V., 2006, Exergoeconomic analysis of gas turbine power plants, *International Energy Journal 7*, 35-41.

Haydargil, D. and Abuşoğlu, A., 2018, A comparative thermoeconomic cost accounting analysis and evaluation of biogas engine-powered cogeneration. *Energy*, *159*, 97-114.

Jung, J. Y., Lee, H. S., Kim, H. J., Yoo, Y., Choi, W. Y. and Kwak, H. Y., 2016, Thermoeconomic analysis of an ocean thermal energy conversion plant. *Renewable Energy*, *86*, 1086-1094.

Keçebaş, A., 2013, Effect of reference state on the exergoeconomic evaluation of geothermal district heating systems. *Renewable and Sustainable Energy Reviews*, *25*, 462-469.

Kecebas, A., 2013, The modified productive structure analysis of Afyon geothermal district heating system for economic optimization. *International Journal of Renewable Energy Research (IJRER)*, *3*(1), 60-67.

Kim, S. M., Oh, S. D., Kwon, Y. H. and Kwak, H. Y., 1998, Exergoeconomic analysis of thermal systems. *Energy*, *23*(5), 393-406.

Kwak, H. Y., Byun, G. T., Kwon, Y. H., and Yang, H., 2002, Cost Structure of CGAM Cogeneration System. In *ASME 2002 International Mechanical Engineering Congress and Exposition* (pp. 225-232). American Society of Mechanical Engineers Digital Collection.

Kwak, H. Y., Lee, H. S., Jung, J. Y., Jeon, J. S. and Park, D. R., 2004, Exergetic and thermoeconomic analysis of a 200-kW phosphoric acid fuel cell plant. *Fuel*, *83*(14-15), 2087-2094.

Kwak, H. Y., Kim, D. J. and Jeon, J. S., 2003, Exergetic and thermoeconomic analyses of power plants. *Energy*, *28*(4), 343-360.

Kwak, H. Y., You, Y., Oh, S. D. and Jang, H. N., 2014, Thermoeconomic analysis of ground-source heat pump systems. *International journal of energy research*, *38*(2), 259-269.

Lazzaretto, A. and Tsatsaronis, G., 2006, SPECO: a systematic and general methodology for calculating efficiencies and costs in thermal systems. *Energy*, *31*(8-9), 1257-1289.

Lozano, M.A., Valero, A., 1993, Thermoeconomic analysis of gas turbine cogeneration systems, Thermodynamics and the Design, Analysis, and Improvement of Energy Systems (Edt. H.J. Richter) 30, 311-320.

Sahu, M. K., Choudhary, T. and Sanjay, Y., 2017, *Exergoeconomic Analysis of Air Cooled Turboprop Engine: Air Craft Application* (No. 2017-01-2044). SAE Technical Paper.

Seo, S. H., Oh, S. D., Oh, H., Kim, M., Lee, W. Y. and Kwak, H. Y., 2019, Thermal management for a hydrogen-fueled 1-kW PEMFC based on thermoeconomic analysis. *International Journal of Hydrogen Energy*, *44*(45), 24934-24946.

Turgut, E. T., Karakoc, T. H. and Hepbasli, A., 2009, Exergoeconomic analysis of an aircraft turbofan engine. *International Journal of Exergy*, *6*(3), 277-294.

Uysal, C., 2020, A new approach to advanced exergoeconomic analysis: The unit cost of entropy generation. *Environmental Progress & Sustainable Energy*, *39*(1), 13297.

Uysal, C., Kurt, H. and Kwak, H. Y., 2017, Exergetic and thermoeconomic analyses of a coal-fired power plant. *International Journal of Thermal Sciences*, *117*, 106-120.

Uysal, C., Ozen, D. N., Kurt, H. and Kwak, H. Y., 2020, A comparative assessment of SPECO and MOPSA on costing of exergy destruction. *International Journal of Exergy*, *32*(1), 62-81.

Yilmaz, C., 2018, Thermoeconomic cost analysis and comparison of methodologies for Dora II binary geothermal power plant. *Geothermics*, *75*, 48-57.

Yoo, Y., Oh, H. S., Uysal, C. and Kwak, H. Y., 2018, Thermoeconomic diagnosis of an air-cooled air conditioning system. *International Journal of Exergy*, *26*(4), 393-417.